Journal of Inorganic Biochemistry 201 (2019) 110820

Contents lists available at ScienceDirect

Journal of Inorganic Biochemistry

journal homepage: www.elsevier.com/locate/jinorgbio

Synthesis and *in vitro* antitumor activity evaluation of copper(II) complexes with 5-pyridin-2-yl-[1,3]dioxolo[4,5-*g*]isoquinoline derivatives

Yun-Liang Zhang[a,b], Cai-Xing Deng[a], Wen-Feng Zhou[a], Liu-Yan Zhou[a], Qian-Qian Cao[a], Wen-Ying Shen[a], Hong Liang[a,*], Zhen-Feng Chen[a,*]

[a] State Key Laboratory for Chemistry and Molecular Engineering of Medicinal Resources, School of Chemistry and Pharmacy, Guangxi Normal University, 15 Yucai Road, Guilin 541004, People's Republic of China
[b] College of Pharmacy, Shaoyang University, Shaoyang, Hunan 422000, People's Republic of China

ARTICLE INFO

Keywords:
Isoquinoline derivatives
Cu(II) complexes
Cell apoptosis
Antitumor activity
Telomerase activity

ABSTRACT

Seven Cu(II) complexes with 5-pyridin-2-yl-[1,3]dioxolo[4,5-*g*]isoquinoline derivatives as ligands: $[Cu_2(\mathbf{L^1})_2Cl_4]$ (**1**), $[Cu(\mathbf{L^2})Cl_2]$ (**2**), $[Cu(\mathbf{L^1})(NO_3)_2]$ (**3**), $[Cu(\mathbf{L^2})(NO_3)_2]$ (**4**), $[Cu(\mathbf{L^3})Cl_2]$ (**5**), $[Cu(\mathbf{L^3})Br_2]$ (**6**) and $[Cu(\mathbf{L^3})(NO_3)_2]$ (**7**){$\mathbf{L^1}$ = 9-nitro-5-pyridin-2-yl-[1,3]dioxolo[4,5-*g*]isoquinoline, $\mathbf{L^2}$ = 4-nitro-5-pyridin-2-yl-[1,3]dioxolo[4,5-*g*]isoquinoline, $\mathbf{L^3}$ = 9-bromo-5-pyridin-2-yl-[1,3]dioxolo[4,5-*g*]isoquinoline}, were synthesized and characterized. Their *in vitro* anticancer activities against T-24, MGC-80-3, HeLa, Hep-G2, A549 and SK-OV-3 were evaluated. Compared with their corresponding ligands, most of these complexes exhibited enhanced anticancer activities in contrast to their corresponding ligands and copper salt. Among them, complexes **1** and **3** displayed selective cytotoxicity to HeLa cells comparing with normal liver cell HL-7702, with IC_{50} values of 5.03 ± 1.20 μM and 10.05 ± 0.52 μM, respectively. Complexes **1** and **3** inhibited telomerase activity by interacting with c-myc promoter elements, and therefore exerted their antitumor activity. Furthermore, complexes **1** and **3** could trigger cell apoptosis via disruption of mitochondrial pathway through notably increased reactive oxygen species (ROS) levels, loss of mitochondrial membrane potential ($\Delta\psi_m$), increase of the cytochrome *c* and apaf-1, decrease of bcl-2, and activation of caspases 3/9. Complexes **1** and **3** exhibited enhanced cytotoxicity, presenting synergetic effect after the ligands coordinated to copper(II) center.

1. Introduction

Telomerase is strongly over-expressed in 85–90% of human cancer cells compared to normal somatic cells [1–5]. Being a specific tumor marker, the enzyme telomerase represents a highly selective anticancer target [6–9]. The transcription factor c-myc gene plays an important role in affecting cellular proliferation, cell growth, as well as apoptosis [2,6,10,11]. Meanwhile, hTERT (human telomerase reverse transcriptase) [8,11,12], as another major component of the human telomerase, is crucial for the regulation of telomere length. Therefore, it is a promising strategy to design and synthesize small molecules stabilizing the G-quadruplex conformation in telomeric DNA or inhibiting telomerase [1,3,5,12–20].

In the past decades, an increasing number of bioactive ligands and their transition metal complexes have been reported as novel and potent telomerase inhibitors. These bioactive ligands mostly contain a planar heteroaromatic moiety, such as berberine [16–18], sanguinarine [16], ethidium derivatives [19], quinoline derivatives [20–22], and isoquinoline derivatives [18,23,24]. The Ni(II) [25,26], Cu(II) [27,28], Ru(II) [29,30] and Pt(II) complexes [31–33] with various bioactive ligands have been reported as potential telomerase inhibitors or G-quadruplex ligands with highly selective antitumor activity.

Among these bioactive ligands, isoquinoline derivatives are the excellent chelators with various pharmacological activities, such as antibacterial, antifungal and anticancer activities [23,24,34–36]. On other hand, copper is one of the most important metal ions in biological systems and a component of many enzymes and proteins [37]. Recently, an impressive number of copper(II) complexes with biological activities, such as antibacterial and antitumor properties have been reported [38–42]. Lots of copper complexes have been reported that copper distribution is much higher in wide spectrum of tumor cells than that in normal cells, and copper may be less toxic for normal cells with respect to cancer cells [41,42]. Therefore, it is a promising therapeutic strategy to explore copper-based complexes as antitumor agents. In recent years, more and more isoquinoline metal complexes have been reported as potential anticancer agents [33,43–45]. Previously, our

* Corresponding author.
E-mail addresses: hliang@gxnu.edu.cn (H. Liang), chenzf@gxnu.edu.cn (Z.-F. Chen).

https://doi.org/10.1016/j.jinorgbio.2019.110820
Received 23 May 2019; Received in revised form 16 August 2019; Accepted 1 September 2019
Available online 02 September 2019
0162-0134/

group has reported a number of antitumor metal complexes with isoquinoline alkaloids such as liriodenine, oxoglaucine, 4,5-methylenedioxy-1-pyridinedihydroisoquinoline and 5-pyridin-2-yl- [1,3]dioxolo [4,5-*g*]isoquinoline [32,45–51]. There is still a need to discover isoquinoline derivatives complexes with high telomerase inhibitory activity [33,52] and high potential as anticancer agents.

In addition, there are some nitro compounds displayed remarkable biological activities [53–56]. Some complexes containing nitro compounds as ligands have been reported with good anticancer activities [57,58]. Hence, to continue our previous study on the 5-pyridin-2-yl-[1,3]dioxolo[4,5-g] isoquinoline derivatives and their metal complexes as anticancer agents, we introduced one substituent (nitro group or Br) to the aromatic ring and synthesized three new 5-pyridin-2-yl- [1,3] dioxolo[4,5-*g*]isoquinoline derivatives. We synthesized and characterized seven new copper(II) complexes of isoquinoline derivatives, evaluated their cytotoxicity and determined cell apoptosis as well as their inhibitory effects on telomerase.

2. Results and discussion

2.1. Synthesis and characterization

5-Pyridin-2-yl-[1,3]dioxolo[4,5-*g*]isoquinoline ($\mathbf{L^0}$) was prepared using our previously reported method [48]. The synthetic route for ligands $\mathbf{L^1}$-$\mathbf{L^3}$ ($\mathbf{L^1}$ = 9-nitro-5-pyridin-2-yl-[1,3]dioxolo[4,5-*g*]isoquinoline, $\mathbf{L^2}$ = 4-nitro-5-pyridin-2-yl-[1,3]dioxolo[4,5-*g*]isoquinoline, $\mathbf{L^3}$ = 9-bromo-5-pyridin-2-yl-[1,3]dioxolo[4,5-*g*]isoquinoline) and their copper(II) complexes **1–7** are shown in Scheme 1. Ligands $\mathbf{L^1}$ and $\mathbf{L^2}$ were prepared using KNO_3-H_2SO_4 at low temperatures [59], while $\mathbf{L^3}$ was synthesized according to the reported methods [60]. Seven copper (II) complexes were obtained by reaction of copper(II) salts with the corresponding ligands ($\mathbf{L^1}$, $\mathbf{L^2}$, $\mathbf{L^3}$) in the presence of CH_3OH and $CHCl_3$/CH_2Cl_2/DMSO at appropriate temperature for several days. These compounds were characterized by ESI-MS, IR, UV-Vis, elemental analysis, single-crystal X-ray diffraction analysis (except for $\mathbf{L^3}$), ^1H and ^{13}C NMR (for $\mathbf{L^1}$ -$\mathbf{L^3}$). The complexes are formulated as: $[Cu_2(\mathbf{L^1})_2Cl_4]$ (**1**), $[Cu(\mathbf{L^2})Cl_2]$ (**2**), $[Cu(\mathbf{L^1})(NO_3)_2]$ (**3**), $[Cu(\mathbf{L^2})(NO_3)_2]$ (**4**), $[Cu(\mathbf{L^3})Cl_2]$ (**5**), $[Cu(\mathbf{L^3})Br_2]$ (**6**) and $[Cu(\mathbf{L^3})(NO_3)_2]$ (**7**). All important data and results are given in the experimental section and supporting information materials in Figs. S1–S28.

2.2. Structure of L^1, L^2, L^3 and Cu(II) complexes 1–7

The crystal structures of $\mathbf{L^1}\mathbf{L^2}$, complexes **1–7** and the chemical structure of $\mathbf{L^3}$ are depicted in Figs. 1 and 2, respectively. The crystallographic data and refinement details for $\mathbf{L^1}$, $\mathbf{L^2}$ and complexes **1–7** are summarized in the Supporting Information (Tables S1-S4). As shown in Fig. 2 (A), with the similar structure of isoquinoline Cu(II) complex $Cu_2(\mathbf{L^0})_2Cl_4$ [48], complex **1** is a binuclear structure linked by two μ-Cl. Each Cu(II) is coordinated with one terminal Cl^-, two μ-Cl anions, and two N from one bidentate $\mathbf{L^1}$, adopting a five-coordinated slightly distorted square-pyramid geometry. The Cu···Cu separation is 3.6359(19) Å, implying very weak metal-metal interaction. It can be found that complex **1** exists in a tetra-coordinated mononuclear form ($[Cu(\mathbf{L^1})Cl + DMSO]^+$) (shown as Fig. S10) with the chlorine bridge broken, when dissolved in a polar solution (DMSO/methanol/H_2O). Thus, we can propose that two μ-Cl bonds in complex **1** are weak and easily broken. Such structural feature provide the possibility for complex **1** covalently binding to biological molecules and responsible for its various cytotoxicity [48,50,51].

The crystal structures of complexes **2**, **3**, **4**, **5**, **6**, **7** are shown in Fig. 2(B), (C), (D), (E), (F) and (G), respectively. Selected bond angle and bond length data are listed in Table S4. The copper centers in complexes **2** to **7** all are tetra-coordinated with one bidentate chelating $\mathbf{L^1}$/$\mathbf{L^2}$/$\mathbf{L^3}$ (via N1, N2 atoms) and two monodentate anions (Cl^-/Br^-/NO_3^-), forming a nearly square-planar geometry. In complexes **2–7**, all bond lengths of Cu—N, Cu—O, Cu—Cl and Cu—Br are in the ranges of 1.969–2.048, 1.960–1.981, 2.014–2.2385 and 2.340–2.369 Å, respectively, which are within the normal range [48,50,61,62].

2.3. Stability and solubility studies of Cu(II) complexes 1–7

The stability of $\mathbf{L^1}$-$\mathbf{L^3}$ and complexes **1–7** (1.0×10^{-5} M) in 10 mM Tris-HCl buffer solution (TBS, pH = 7.35, containing 1.0% DMSO) were measured by following the changes in the UV–visible spectroscopy as shown in Fig. S27. The time-dependent (0 h, 24 h and 48 h) UV–Vis spectra of the tested compounds revealed slight hypochromicity but no remarkable shift over time, indicating that these complexes were stable in Tris-HCl buffer solution for 48 h at room temperature. In addition, their stabilities were further investigated by HPLC. As depicted in Fig. S28, the retention time for all compounds remained unchanged under the same conditions (mobile phase: 90:10 or 80:20 methanol/H_2O), which showed that complexes **1–7** were stable for 48 h in DMSO stock solution. The results suggested that complexes **1–7** were stable in TBS and DMSO solution. Further confirmed by ESI-MS, complex **1** was existed as mononuclear species because it was dissociated in solution (Fig. S10).

In addition, the water solubility of complexes **1–7** was determined gravimetrically by UV spectroscopy (containing 2.0% DMSO), as shown in Fig. S29 [63,64]. The solubility of complexes **1–7** in distilled water was similar, with the solubility of 1.62, 1.75, 1.40, 1.30, 1.30, 1.35 and 1.60 mg/mL at room temperature, respectively. The results showed that the solubility could provide an appropriate concentration for the biological experiments under near physiological conditions.

2.4. In vitro cytotoxicity

The *in vitro* cytotoxicities of complexes **1–7**, $\mathbf{L^1}$-$\mathbf{L^3}$, and $CuCl_2{\cdot}2H_2O$/$Cu(NO_3)_2{\cdot}2H_2O$/$CuBr_2$ were evaluated against six human cancer cell lines (T-24, MGC-80-3, HeLa, Hep-G2, A549 and SK-OV-3) and one normal tumor cell (HL-7702) by 3-(4,5-dimethylthiazol-2-yl)-2,5-diphenyltetrazolium bromide (MTT) assay, using cisplatin as the positive control. Table 1 and Table S5 show that complexes **1–7** exhibited higher cytotoxicity than $\mathbf{L^1}$, $\mathbf{L^2}$, $\mathbf{L^3}$ (except for Hep-G2) and the corresponding copper(II) salts, which implied the existence of synergistic effects after the ligands coordinated to copper(II). Among them, complexes **1** and **3**, especially complex **1**, exhibited higher anticancer activity against most of the tested human tumor cell lines, with lower IC_{50} values (IC_{50} = 5.03–15.86 μM). In general, the *in vitro* antitumor activities of complexes **1–7** against HeLa cells were related to 4 or 9-substuted-5-pyridine-2-yl-[1,3]dioxolo[4,5-*g*]isoquinoline following the order of **1** > **3** > **5** > **2** > **4** > **6**. Notably, complexes **1** and **3**

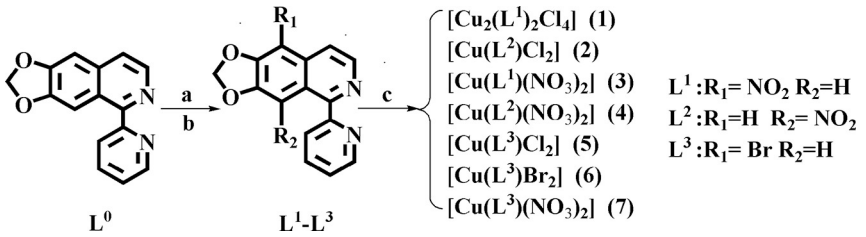

Scheme 1. Synthetic routes for 5-pyridin-2-yl-[1,3]dioxolo [4,5-*g*] isoquinoline derivatives, which are 9-Nitro-5-pyridin-2-yl-[1,3]dioxolo[4,5-*g*] isoquinoline ($\mathbf{L^1}$), 4-Nitro-5-pyridin-2-yl-[1,3]dioxolo[4,5-*g*]isoquinoline ($\mathbf{L^2}$), and 9-Bromo-5-pyridin-2-yl-[1,3]dioxolo[4, 5-*g*]isoquinoline ($\mathbf{L^3}$), and complexes **1–7** Reagents are as follows: a: $\mathbf{L^1}$ -$\mathbf{L^2}$: KNO_3, H_2SO_4, 0 °C; b: $\mathbf{L^3}$: Br_2, $CHCl_3$, 40 °C; c: Salts: $CuCl_2{\cdot}2H_2O$/$Cu(NO_3)_2{\cdot}2H_2O$/$CuBr_2{\cdot}2H_2O$; Solvent: CH_3OH and $CHCl_3$/DMSO: Temperature: 40 °C/60 °C/80 °C.

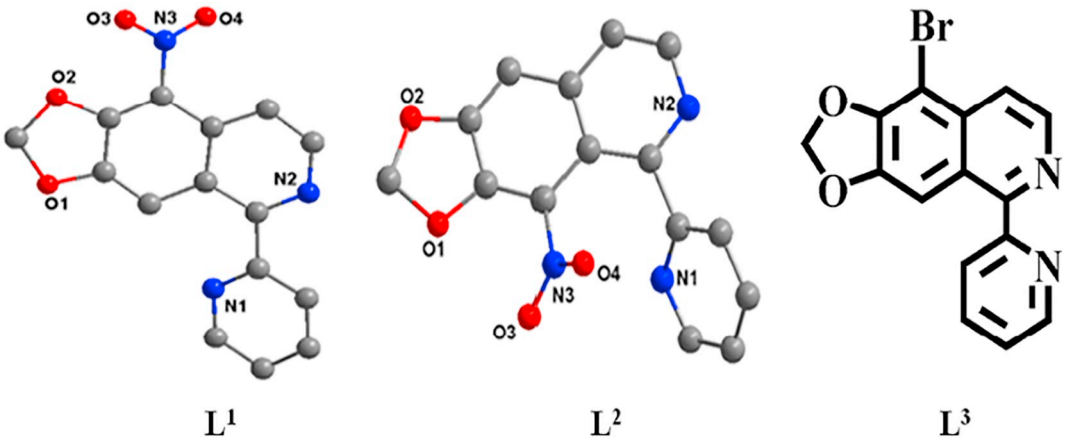

Fig. 1. Chemical structures of ligands L^1 -L^3. Hydrogen atoms are omitted for clarity.

showed remarkable cytotoxicity (IC_{50} = 5.03 and 10.05 μM) in HeLa cells, which was 3.0 times and 1.5 times more active than that of cisplatin (IC_{50} = 15.09 ± 0.74 μM), respectively.

As shown in Table 1, comparing L^1(-NO_2 in 9-position)moiety to L^3 (-—Br in 9-position), L^1 showed more effective activity against T-24, HeLa, A549, SK-OV-3 than L^3, which is similar to the results reported by Duan [22]. The result is understandable as NO_2 is a good pharmacophore. While comparing L^1 with L^2 (-NO_2 in 4-position), L^1 exhibited higher cytotoxicity on cancer cells than L^2, which may be attributed to their steric factors. Interestingly, complex **1** and complex **3**, although having different coordination geometry, both displayed stronger anticancer activities than the other complexes containing L^2 and L^3, with the activity order of complex **1** > complex **3**. On the other hand, complex **3** and complex **4** although having similar coordination geometry, complex **4** showed weaker *in vitro* cytotoxicity than complex **3**, against the most of the tested cancer cells. All the results clearly hint that the existence of L^1 in complexes plays a key role to enhance the anticancer activities in complexes **1** and **3**. The coordination of L^1-L^3 to Cu(II) center to form complexes **1–7** enhanced their anticancer activity against three or more of the used tumor cells, suggesting a synergistic effect.

In addition, compared the data in Table 1 with those previously reported data on L^0 and $Cu_2(L^0)_2Cl_4$ [48], it was found that complex **1** only showed little higher *in vitro* cytotoxicity against SK-OV-3 tumor cells, showing lower cytotoxicity to A549 and MGC-80-3 than $Cu_2(L^0)_2Cl_4$. Basing on these results, it can be speculated that the antitumor activity of similar Cu(II) complexes could not be enhanced with nitro groups introduced to L^0, The nitro may destroy the binding with the targeting molecules.

2.5. Cellular uptake and distribution of metals in HeLa cells

The MTT assay data showed that complex **1** and complex **3** displayed more potent anticancer activities on HeLa tumor cells than the other complexes, especially complex 1. To better understand the complexes **1** and **3**-mediated cytotoxic activity and cell apoptosis, the uptake and distribution of Pt, Cu in HeLa cells were investigated using inductively coupled plasma mass spetrometry (ICP-MS) assay, using

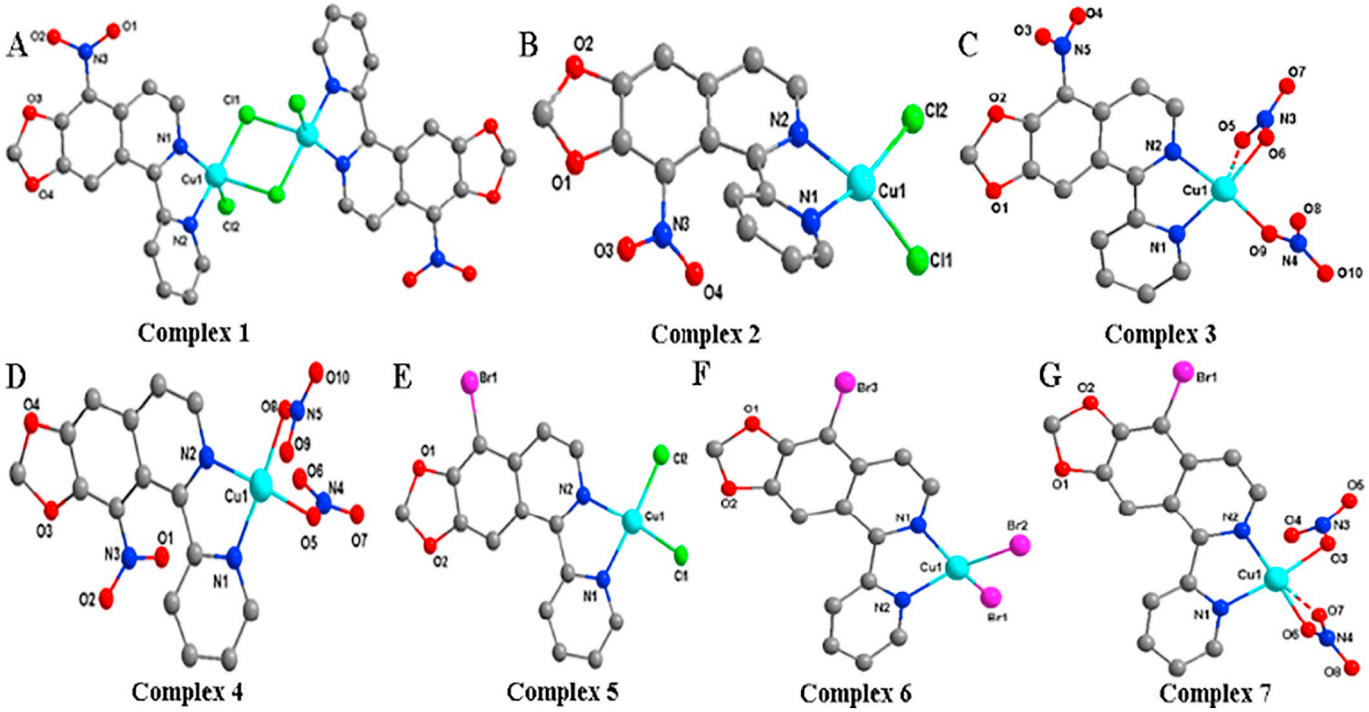

Fig. 2. Perspective view of complexes **1**(A), **2** (B), **3**(C), **4**(D), **5**(E), **6**(F) and **7**(G). Hydrogen atoms are omitted for clarity.

Table 1
IC_{50}[a] (μM) values of complexes **1–7**, $\mathbf{L^1}$ -$\mathbf{L^3}$ and cisplatin to six selected human tumor and one normal cells.

Compds	T-24	MGC-80-3	HeLa	Hep-G2	A549	SK-OV-3	HL-7702
1	9.02 ± 0.31	5.62 ± 1.27	5.03 ± 1.20	5.39 ± 0.71	6.47 ± 1.06	14.06 ± 0.54	28.06 ± 1.46
2	23.28 ± 0.72	19.05 ± 0.51	25.24 ± 1.12	16.49 ± 0.52	28.97 ± 0.85	> 100	35.85 ± 0.36
3	15.40 ± 0.92	17.91 ± 0.38	10.05 ± 0.52	15.86 ± 0.45	6.03 ± 1.02	> 100	30.16 ± 0.63
4	27.64 ± 1.05	26.95 ± 0.17	33.46 ± 0.82	18.73 ± 1.12	28.29 ± 1.03	> 100	39.86 ± 0.59
5	14.49 ± 0.87	31.10 ± 1.32	23.27 ± 1.31	13.42 ± 1.23	10.29 ± 0.62	72.38 ± 1.20	39.89 ± 1.29
6	21.49 ± 1.05	11.46 ± 1.03	34.71 ± 1.55	26.04 ± 1.69	13.14 ± 1.08	> 100	34.15 ± 1.42
7	20.92 ± 0.60	15.58 ± 2.05	49.53 ± 1.59	8.59 ± 1.95	10.99 ± 1.39	25.55 ± 0.72	36.45 ± 0.74
$\mathbf{L^1}$	43.70 ± 1.70	34.97 ± 0.73	33.63 ± 1.83	17.97 ± 1.19	34.49 ± 1.03	66.13 ± 1.62	> 100
$\mathbf{L^2}$	93.30 ± 0.79	42.31 ± 0.51	> 100	> 100	> 100	> 100	> 100
$\mathbf{L^3}$	63.56 ± 0.75	26.08 ± 1.11	> 100	11.96 ± 1.05	63.62 ± 0.87	> 100	> 100
Cisplatin[b]	14.03 ± 1.12	15.07 ± 0.78	15.09 ± 0.74	11.23 ± 1.02	10.25 ± 1.05	13.25 ± 0.81	18.09 ± 0.34

[a] IC_{50} values are presented as the mean. SD (standard error of the mean) from five or six independent experiments.
[b] Cisplatin was dissolved at a concentration of 1.0 mM in 0.154 M NaCl [64,65].

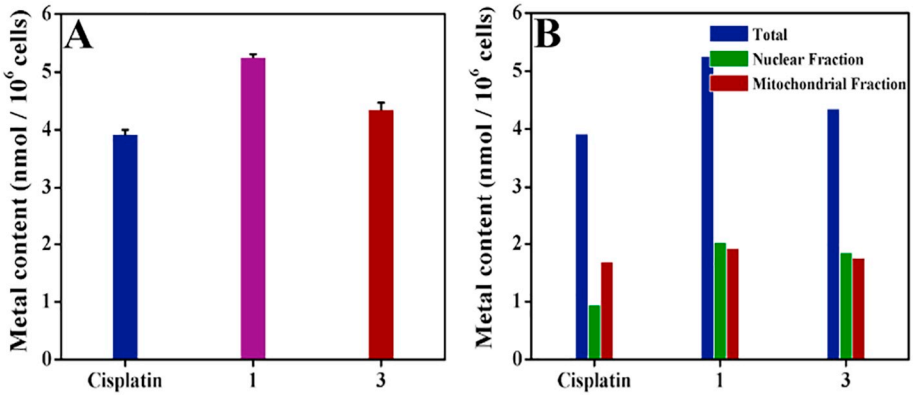

Fig. 3. Metal contents in whole HeLa cells (A) and in different fractions (B) after treated with complex **1** (5.0 μM), **3** (10.0 μM) and cisplatin (15.0 μM) for 24 h by means of ICP -MS.

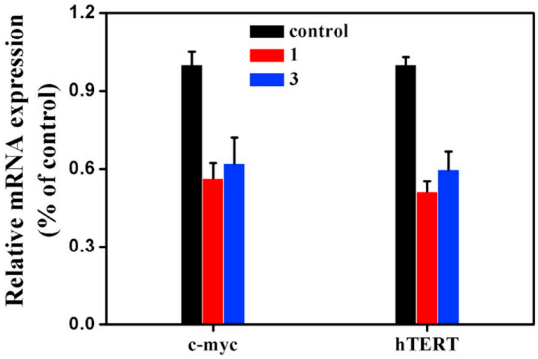

Fig. 4. The expressions of c-myc and hTERT in HeLa cells was determined after treated with complexes **1** (5.0 μM) and **3** (10.0 μM) for 24 h by RT-PCR.

cisplatin as positive control. The nuclear fraction, mitochondrial membrane fraction and cytoplasm fraction were separated and extracted after the HeLa cells were treated with complexes **1** (5.0 μM), **3** (10.0 μM) and cisplatin (15 μM) for 24 h. As depicted in Fig. 3A, complex **1** (5 μM) was significantly accumulated ((5.26 ± 0.05 nmol Cu)/10^6 cells) in the HeLa cells, whereas cisplatin (15.0 μM) and complex **3** (10.0 μM) showed much less accumulation, with contents of (3.92 ± 0.08 nmol Pt)/10^6 cells and (4.35 ± 0.12 nmol Cu)/10^6 cells, respectively. The cell uptake of Cu in HeLa cells in complex **1** was higher than that in complex **3**, probably benefit to improve its cytotoxicity.

In addition, the distributions of complexes **1** (5.0 μM), **3** (10.0 μM) and cisplatin (15.0 μM) in HeLa tumor cells were further investigated using the method reported by Chen and Qin [30,65]. As shown in Fig. 3B, complexes **1** (5.0 μM) and **3** (10.0 μM) were mainly accumulated in nuclear fraction and mitochondrial fraction, whereas cisplatin (15.0 μM) was mainly accumulated in mitochondrial fraction. The different accumulation and distribution of Cu and Pt metals in HeLa cells can be contributed to the different uptake and efflux of cisplatin, complexes **1** and **3**, which may underlie the differences in cell apoptotic pathways they activated [30].

2.6. Effects of complexes 1 and 3 on the expression of c-myc and hTERT genes and proteins

Recent studies have revealed that the expressions of c-myc and hTERT genes may be vital for the telomerase activity [27,65–67]. To study the effects of complexes **1** (5.0 μM) and **3** (10.0 μM) on the expression of c-myc and hTERT genes and proteins in HeLa cells, real-time RT-PCR experiment was firstly used to verify that complexes **1** (5.0 μM) and **3** (10.0 μM) could down-regulate the mRNA expression of hTERT and c-myc in HeLa cells. After the HeLa cells were exposed to complexes **1** (5.0 μM) and **3** (10.0 μM) for 24 h, the results shown in Fig. 4 demonstrated that complexes **1** (5.0 μM) and **3** (10.0 μM) could significantly reduce the expression of c-myc and hTERT. The levels of c-myc were reduced by 43.7% and 37.9%, respectively, compared with the control, and the levels of hTERT decreased by 48.9% and 40.3%, respectively. Compared with the untreated group, the results indicated that complex **1** (5.0 μM) inhibited the expression of c-myc and hTERT protein levels more effectively than that of complex **3** (10.0 μM). Moreover, the inhibitory activity of complexes **1** (5.0 μM) and **3** (10.0 μM) on the expression of c-myc and hTERT was further confirmed by Western blot. As shown in Fig. 5, notable decreases of the expressions of c-myc and hTERT proteins were observed in the HeLa cells treated with complexes **1** (5.0 μM) and **3** (10.0 μM) for 24 h, which were in accordance with the decreased expressions of the respective genes (c-

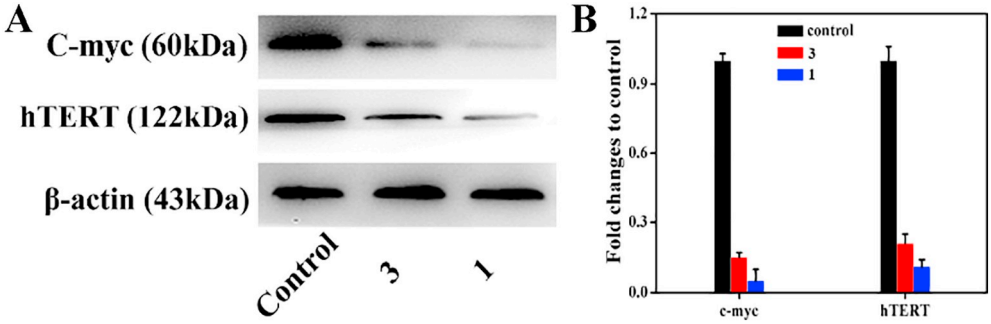

Fig. 5. (A) Western blot analysis of the expression levels of c-myc and hTERT in HeLa cells treated with complexes **1** (5.0 μM) and **3** (10.0 μM) for 24 h. (B) Densitometric analysis of c-myc and hTERT proteins.

myc and hTERT) by RT-PCR experiment.

2.7. Complexes 1 and 3 inhibited the telomerase activity

It is well known that telomerase is strongly over-expressed in 85–90% of all human cancer cells while virtually absent in normal somatic cells [1,2,6,7]. Recently, an increasing number of studies have indicated that telomerase could be an appealing target for drug design and anticancer therapy [1,2,6,7,27,65]. Hence, TRAP-silver staining assay was carried out for complexes **1** and **3**. Fig. 6 revealed that complexes **1** (5.0 μM) and **3** (10.0 μM) could significantly inhibit telomerase activity in HeLa cells with the order of complex **1** > complex **3.** The inhibitory rates of telomerase expression of complexes **1** and **3** reached 44.06% and 40.70%, respectively.

2.8. Measurement of mitochondrial membrane potential ($\Delta\psi_m$)

Recent studies show that mitochondria play a crucial role in the regulation of various apoptosis pathways [64,65]. Cellular uptake study indicated that complexes **1** (5.0 μM) and **3** (10.0 μM) were more effectively accumulated to mitochondrial fraction and nuclear fraction. To establish whether the apoptotic mechanisms induced by complexes **1** and **3** are associated with mitochondrial dysfunction, the alteration in $\Delta\psi_m$ was measured through the examination of complexes **1** (5.0 μM) and **3** (10.0 μM) treated HeLa cells by flow cytometry after staining with 5,5',6,6'-tetra-chloro-1,1'3,3'-tetraethylbenzimidazolylcarbocyanine (JC-1) cationic dye. As shown in Fig. 7, the treatment of HeLa cells with complexes **1** (5.0 μM) and **3** (10.0 μM) for 24 h caused obvious $\Delta\psi_m$ loss comparing with the control (24.3% and 22.70%, respectively), suggesting that the mitochondrial membrane was significantly damaged. The results indicated that the cell apoptosis induced by complexes **1** (5.0 μM) and **3** (10.0 μM) was related to the mitochondrial pathway.

Fig. 6. The inhibition of telomerase activity in HeLa cells treated with complexes **1** (5.0 μM) and **3** (10.0 μM) for 24 h.

2.9. Effect on intracellular ROS generation

An increasing number of anticancer drugs induce the production of reactive oxygen species (ROS) in tumor cells, ultimately inducing cancer cell death and/or apoptosis [64,68,69]. Herein, we investigated the effects of complexes **1** (5.0, 10.0 μM), **3** (10.0 μM) and Cisplatin (15.0 μM) on inducing the production of ROS that could potentially lead to the cytotoxic effect in HeLa cells. The ROS levels were examined by using an oxidant-sensitive fluorescent probe, 2′,7′-dichlorofluorescindiacetate (DCFH-DA). As illustrated in Fig. 8, upon treatment of HeLa cells with complexes **1** (5.0, 10.0 μM), **3** (10.0 μM) and cisplatin (15.0 μM) for 24 h, the levels of ROS (strong green fluorescence observed under a Nikon Te2000 deconvolution microscope) were significantly increased in HeLa cells, which agreed well with the flow cytometric analysis results for ROS generation in HeLa cells (Fig. 9 and Fig. S30). Taken together, these results suggested that complexes **1** (5.0 μM, 10.0 μM) and **3** (10.0 μM) (compared with cisplatin) have induced oxidative imbalance, enhanced the generation of ROS in HeLa cells, and ultimately caused cell apoptosis via mitochondrial pathway [68,70]. The above outcomes are in good agreement with the results of MTT assay, cell uptake assay, telomerase inhibition and mitochondrial membrane potential assay.

2.10. Measurement of Ca^{2+} fluctuation

Recent investigations have confirmed that increases in Ca^{2+} levels mediated by various channels can alter $\Delta\psi_m$ in cancer cells, which is related to cell apoptosis [70,71] just like the deregulation of ROS generation. Thus, we examined the effects of complexes **1** (5.0, 10.0 μM), **3** (10.0 μM) and cisplatin (15.0 μM) on intracellular Ca^{2+} mobilization in HeLa cells via flow cytometry using the fluorescent probe Fluo-3/AM. As shown in Fig. 10 and Fig. S30, after incubated with complexes **1** (5.0, 10.0 μM), **3** (10.0 μM) and cisplatin (15.0 μM) for 24 h, the level of intracellular Ca^{2+} in these cancer cells increased steadily compared with the control. Our findings revealed that the increases of Ca^{2+} levels and accumulation of ROS could induce apoptosis in HeLa cells.

2.11. Determination of cell apoptosis by flow cytometry

Therefore, the apoptotic effects of complexes Cisplatin(15.0 μM) , **1** (5.0 μM) and **3** (10.0 μM) were further evaluated by Annexin V FITC (fluorescein isothiocyanate)/PI (propidium iodide) double staining assay [65,72–74]. After exposure to Cisplatin(15.0 μM) , **1** (5.0 μM) and **3** (10.0 μM) for 24 h, significant apoptosis of HeLa cells was effectively induced, and the population of apoptic cells (Q2 + Q3) were 13.09%, 43.70% and 37.65%, respectively (Fig. 11). Furthermore, the cell apoptotic effect of complex **1** (5.0 μM) was stronger than that of complex **3** (10.0 μM) and cisplatin (15.0 μM).

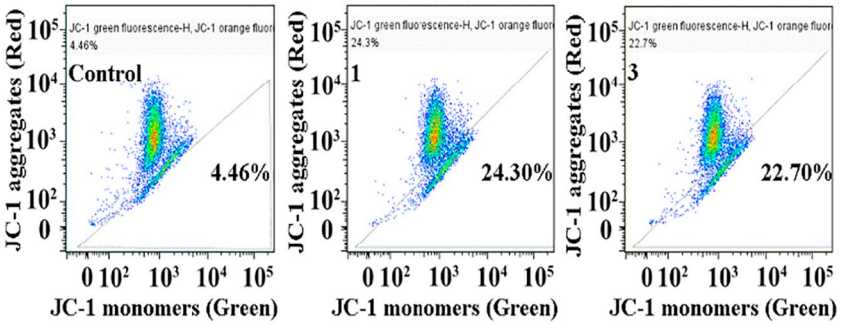

Fig. 7. Loss of Δψ in HeLa cells exposed to complexes **1** (5.0 μM) and **3** (10.0 μM) for 24 h using staining with JC-1, and examined by flow cytometry.

2.12. The expression of apoptosis related proteins in HeLa cells

To further elucidate the molecular mechanisms of the induced apoptosis, we investigated the effects of complexes **1** and **3** on the expression of the important proteins involved in mitochondria mediated apoptosis. As shown in Fig. 12, complexes **1** (5.0 μM) and **3** (10.0 μM) were able to decrease the level of bcl-2, and to increase the levels of apaf-1 and cytochrome *c* in HeLa cells, which were correlated with mitochondrial membrane depolarization and cell apoptosis [45,65,72–76].

2.13. Activation of caspase-3 and caspase-9

The activation of caspase-3 and caspase-9 plays a critical role in the process of programmed cell death or/and apoptosis [45,65,72,73]. To better understand the apoptotic pathway induced by complexes **1** (5.0 μM) and **3** (10.0 μM) in HeLa cells, the expressions of caspase-3/9 were assessed by flow cytometry. As shown in Fig. 13, after treated with complexes **1**, **3** and cisplatin for 24 h, the caspase-3 expression levels were increased from 3.60% to 17.50%, 12.90% and 11.10%, respectively. And the expression of caspase-9 was increased from 2.60% to 9.87%, 7.09% and 5.62%, compared to untreated control, respectively, which confirmed that complexes **1** and **3** induced HeLa cells apoptosis [45,65,73]. These results suggested that complexes **1** and **3** could induce the expression of caspase-3/−9 and cause apoptosis.

3. Conclusion

In this study, $\mathbf{L^1}$-$\mathbf{L^3}$ and their Cu(II) complexes **1–7** have been prepared and fully characterized. We evaluated the *in vitro* cytotoxicity of these compounds against six cancer cell lines by MTT assay. These complexes generally showed enhanced cytotoxicity, demonstrating synergetic effect after the ligands coordinated to copper(II) centre. Moreover, modification of 5-pyridine-2-yl-[1,3]dioxolo[4,5-*g*]isoquinoline with nitro or Br group affected the *in vitro* cytotoxicity, and

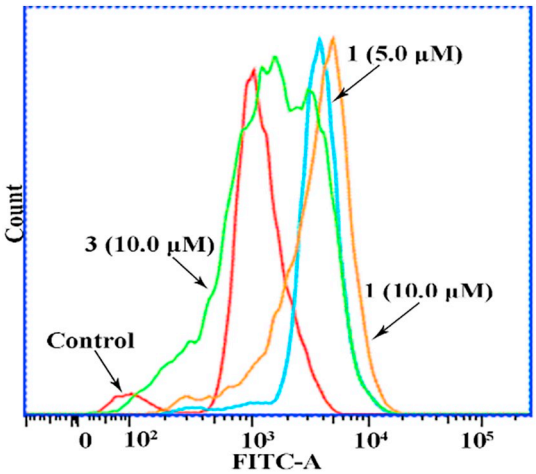

Fig. 9. Measurement of ROS levels by flow cytometric analysis after the HeLa cells were treated with complex **1** (5.0 μM,10.0 μM) and **3** (10.0 μM) for 24 h.

the $\mathbf{L^1}$ - containing complexes exhibited higher activity than $\mathbf{L^3}$- containing complexes in the five tested tumor cell lines. In general, the *in vitro* antitumor activities of complexes **1–7** against HeLa cells followed the order of **1** > **3** > **5** > **2** > **4** > **6**. Notably, complexes **1** and **3** were selectively cytotoxic towards HeLa cells, comparing with human normal live cells (HL-7702). Various *in vitro*assays indicated that complexes **1** and **3** could effectively inhibit telomerase activity by binding to c-myc promoter elements. In addition, complexes **1** and **3** also could induce cell apoptosis via mitochondrial dysfunction.

4. Experimental section

The purity of complexes 1–7 used in our studies was 95%, which was routinely checked by HPLC.

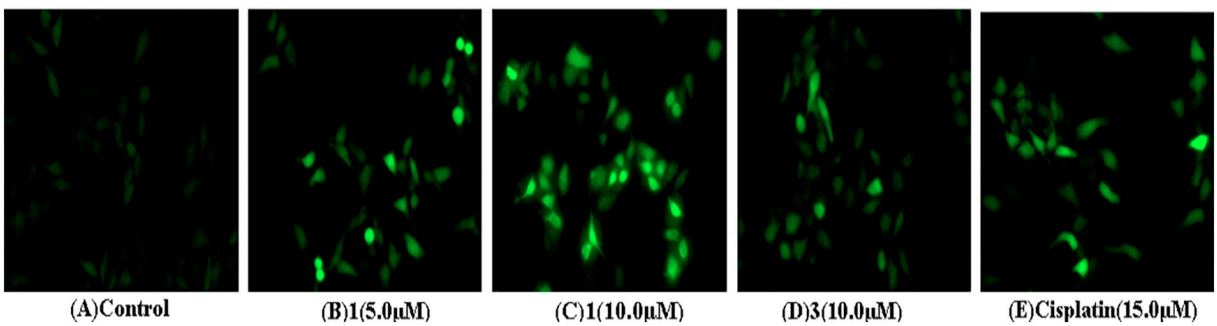

Fig. 8. ROS generation assay in HeLa cells after treatment with complexes **1** (5.0 μM,10.0 μM) and **3** (10.0 μM) for 24 h. Images were obtained using a Nikon Te2000 deconvolution microscope (magnification 20×).

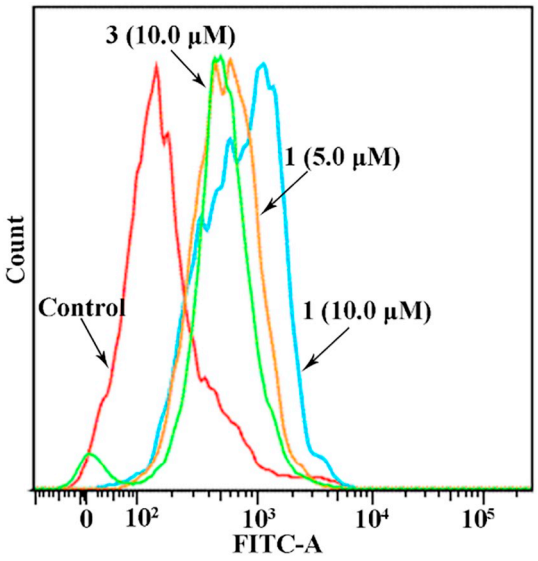

Fig. 10. Effects of complex **1** (5.0, 10.0 μM) and **3** (10.0 μM) on the intracellular Ca^{2+} levels in HeLa cells treated with complex **1** (5.0, 10.0 μM) and complex **3** (10.0 μM) for 24 h, and analyzed by flow cytometry after stained with Fluo-3 AM.

4.1. Synthesis of ligands

The synthesis of 5-pyridin-2-yl-[1,3]dioxolo[4,5-g]isoquinoline ($\mathbf{L^0}$) was performed using the methods as previously reported by Huang [51]. 9-nitro-5-pyridin-2-yl- [1,3] dioxolo[4,5-g]isoquinoline ($\mathbf{L^1}$), 4-nitro-5-pyridin-2-yl-[1,3]dioxolo[4,5-g]isoquinoline ($\mathbf{L^2}$) were prepared as follows: 5-pyridin-2-yl-[1,3]dioxolo[4,5-g]isoquinoline (2.5 g, 10 mmol) in a 250 mL dry flask was stirred in 80 mL of concentrated H_2SO_4 in ice bath before all the solid was dissolved. KNO_3 pellets (1.02 g, 10 mmol, 1.0 equiv) were then slowly added to the above solution [59]. The reaction mixture was stirred at 0 °C for 5 h, then slowly poured onto ice, basified with 5% NaOH aq and stirred for another 30 min. The brown mixture was filtered and washed with cool water (3 × 20 mL). The crude product was purified with silica gel column chromatography using eluent of CH_2Cl_2/petroleum ether to get $\mathbf{L^1}$ and $\mathbf{L^2}$, with 52% and 33% yield, respectively.

Data for $\mathbf{L^1}$: ^{1}H NMR (500 MHz, $CDCl_3$):δ 8.77 (s, 1H, H-8), 8.69 (d, J = 5.8 Hz, 1H, H-3), 8.37–8.34 (m, 1H, H-6′), 8.29 (d, J = 5.7 Hz, 1H, H-4), 8.06 (d, J = 7.7 Hz, 1H, H-3′), 7.96–7.90 (m, 1H, H-4′), 7.46–7.43 (m, 1H, H-5′), 6.33 (s, 2H, H-9). ^{13}C NMR (125 MHz, $CDCl_3$) δ 157.82 (C-1), 155.90 (C-6), 148.62 (C-7), 148.46 (C-6′), 147.33 (C-2′), 144.08 (C-3), 137.34 (C-4′), 128.18 (C-4a), 126.36 (C-5), 125.47 (C-3′), 123.61 (C-5′), 122.90 (C-8a), 115.76 (C-8), 109.12 (C-4), 104.02 (C-9). ESI-MS: m/z 296.0666[M + H]$^+$; Selected IR (KBr, cm^{-1}): 3078, 2923 (ν (Ar—H); 1557 (ν(C=N)); 1519 ($\nu_{as}(NO_2)$); 1338 (ν_s (NO_2)), 892 (ν (C—N)). Anal. Calc. (%) (for $C_{15}H_9N_3O_4$): C 61.02, H 3.07, N 14.23; Found: C 60.86, H 3.28, N 14.30.

Data for $\mathbf{L^2}$: ^{1}H NMR (400 MHz, DMSO-d_6) δ 8.61 (d, J = 5.3 Hz, 1H, H-3), 8.39 (d, J = 7.8 Hz, 1H, H-6′), 8.06 (d, J = 7.9 Hz, 1H, H-3′), 7.98 (dd, J = 7.6, 1.5 Hz, 1H, H-4′), 7.82 (d, J = 5.4 Hz, 1H, H-4), 7.68 (s, 1H, H-5), 7.41–7.38 (m, 1H, H-5′), 6.44 (s, 2H, H-9). ^{13}C NMR (100 MHz, DMSO-d_6) δ 158.95 (C-1), 154.20 (C-7), 151.56 (C-6), 148.08 (C-6′), 146.16 (C-2′), 142.95 (C-3), 137.83 (C-4′), 136.14 (C-4a), 128.03 (C-8), 124.00 (C-3′), 123.41 (C-5′), 120.57 (C-5), 114.66 (C-8a), 106.58 (C-4), 105.36 (C-9). ESI-MS: m/z 296.0661[M + H]$^+$. Selected IR (KBr, cm^{-1}): 3018, 2915 (ν (Ar—H)); 1536 ($\nu_{as}(NO_2)$); 1331 ($\nu_s(NO_2)$); 1575 (ν(C=N)); 894 (ν (C—N)). Anal. Calc. (%) (for $C_{15}H_9N_3O_4$): C 61.02, H 3.07, N 14.23; Found: C 60.93, H 3.02, N 14.26.

In a double necked flask, a solution of Br_2 (0.1 mmol in 15 mL $CHCl_3$, 1.0 eq) was added dropwise to a solution of 5-pyridin-2-yl-[1,3] dioxolo[4,5-g]isoquinoline (0.5 g, 0.2 mmol in 40 mL dry methylene chloride) under nitrogen atmosphere at room temperature [60]. Then the overall mixture was refluxed for 2 h. Afterwards, the vessel content was cooled to room temperature, poured onto ice, alkalinized (pH 9–10) with 5% aqueous NH_4OH and filtered. The resulting solid was washed with ether (2 × 5 mL) to give the crude product. The final product was purified by silica gel column chromatography to obtain white needle-like solid (yield 51%).

Data for $\mathbf{L^3}$: ^{1}H NMR (400 MHz, $CDCl_3$) δ 8.76 (d, J = 4.5 Hz, 1H, H-6′), 8.59 (d, J = 5.7 Hz, 1H, H-3), 7.99–7.97 (m, 2H, H-3′, 4′), 7.92–7.87 (m, 2H, H-3, 8), 7.40–7.37 (m, 1H, H-5), 6.16 (s, 2H, H-9). ^{13}C NMR (100 MHz, $CDCl_3$) δ 158.41 (C-1), 156.01 (C-7), 149.16 (C-6), 148.63(C-6′), 148.14(C-2′), 142.49 (C-2), 137.20 (C-4′), 134.59 (C-4a), 125.43 (C-3′), 124.66(C-8a), 123.40 (C-5′), 118.99(C-4), 103.54 (C-8), 102.05 (C-9), 96.27 (C-5). ESI – MS: m/z 330.9900 [M + H]$^+$. Selected IR (KBr, cm^{-1}): 2919 (ν(Ar—H); 1562 (ν(C=N)); 829 (ν(C—Br)). Anal. Calc. (%) (for $C_{15}H_9BrN_2O_2$): C 54.74, H 2.75, N 8.51; Found: C 54.47, H 2.68, N 8.62.

4.2. Synthesis of complexes 1–7

A mixture of corresponding copper(II) salts (0.1 mmol, $CuCl_2{\cdot}2H_2O$/ $Cu(NO_3)_2{\cdot}2H_2O$/$CuBr_2$, respectively) , ligand $\mathbf{L^1}$/$\mathbf{L^2}$/$\mathbf{L^3}$ (0.1 mmol), methanol and $CHCl_3$/DMSO was placed in a thick Pyrex tube (ca. 25 cm long). The resulting mixture was frozen by liquid N_2 and vacuumed, sealed, and then heated at the appropriate temperature for 3–5 days. After that, the mixture was slowly cooled to room temperature at a rate of 5 °C/h to obtain crystals of complexes **1–4**, **6,7** suitable for single crystal X-ray diffraction analysis.

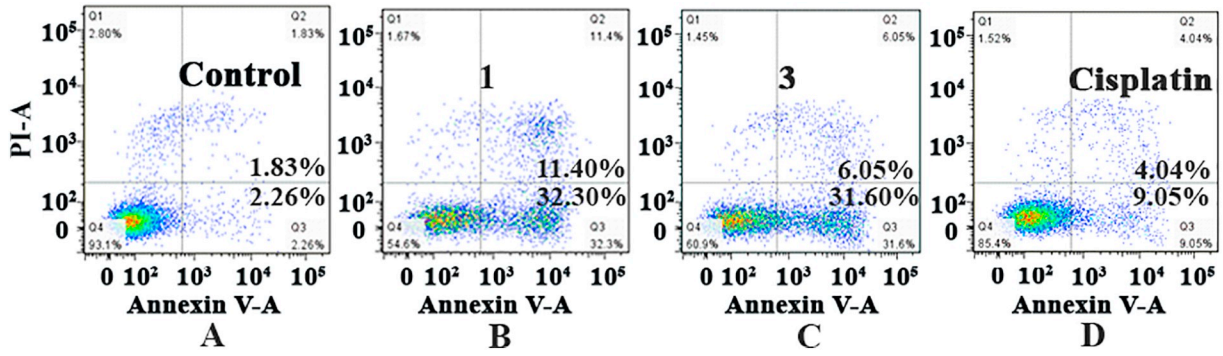

Fig. 11. Apoptosis of HeLa cells treated with **1** (5 0 μM) and **3** (10.0 μM) for 24 h by staining with Annexin V/propidium iodide, compared with the control group.

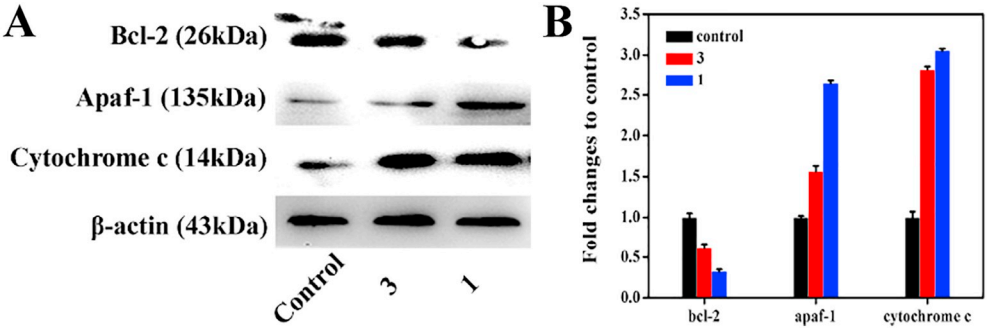

Fig. 12. (A) Western blot assay was used to determine the expression of cytochrome *c*, apaf-1 and bcl-2 in HeLa cells treated with complexes **1** (5 μM) and **3** (10.0 μM) for 24 h. (B) Densitometric analysis of cytochrome *c*, apaf-1 or bcl-2 protein normalized with β-actin. The relative expression of each protein is represented by the density of the protein band/density of β-actin band. Mean SD was from three independent measurements.

Data for complex 1: $CuCl_2{\cdot}2H_2O$(0.1 mmol, 0.0171 g), $\mathbf{L^1}$ (0.1 mmol, 0.0295 g), methanol (1.0 mL) and dimethyl sulfoxide (0.2 mL) was placed in a thick Pyrex tube (ca. 25 cm long).The resulting mixture was frozen by liquid N_2 and vacuumed, sealed, and then heated at 80 °C for 3 days. The green block crystals were used for single crystal X-ray diffraction analysis. Yield (65%). ESI – MS: 470.97 $[Cu(\mathbf{L^1})Cl + DMSO]^+$; Selected IR (KBr, cm^{-1}): 3105, 2923 (ν(Ar—H); 1574 (ν(C=N)); 1536 ($\nu_{as}(NO_2)$); 1335 ($\nu_s(NO_2)$); 874 (ν(C—N)). Anal. Calc. (%) (for $C_{30}H_{18}Cl_4Cu_2N_6O_8$): C 41.93, H 2.11, N 9.78; Found: C 41.81, H 2.03, N 9.83.

Data for complex 2: According to the similar procedure, complex **2** was gained from $CuCl_2{\cdot}2H_2O$ (0.1 mmol, 0.0171 g), $\mathbf{L^2}$ (0.1 mmol, 0.0295 g), methanol (1.0 mL) and $CHCl_3$ (0.2 mL), with the reaction solution heated at 40 °C. The blue-green block crystals were used for single crystal X-ray diffraction analysis. Yield 67%. ESI-MS: 470.97 $[Cu(\mathbf{L^2})Cl + DMSO]^+$; Selected IR (KBr, cm^{-1}): 2926 (ν(Ar—H)); 1577 (ν(C=N)); 1524 ($\nu_{as}(NO_2)$); 1329 ($\nu_s(NO_2)$; 884 (ν(C—N)). Anal. Calc. (%) (for $C_{15}H_9Cl_2CuN_3O_4$): C 41.93, H 2.09, N 9.78; Found: C 41.91, H 2.08, N 9.81.

Data for complex 3: Using a similar process as complex **1**, complex **3** was obtained from the mixture of $Cu(NO_3)_2{\cdot}2H_2O$(0.0223 g), $\mathbf{L^1}$ (0.1 mmol, 0.0295 g), methanol(1.0 mL) and $CHCl_3$ (0.2 mL) as a green rod-shaped crystal. Yield 73%. ESI-MS: *m/z* 419.97 $[Cu(\mathbf{L^1})(NO_3)]^+$, *m/z* 497.97 $[Cu(\mathbf{L^1})(NO_3) + DMSO]^+$; Selected IR (KBr, cm^{-1}): 3105, 2925 (ν(Ar—H)); 1579 (ν(C=N)); 1529 ($\nu_{as}(NO_2)$); 1258 (ν_s (NO_2)); 1383 ($\nu(NO_3^-)$), 805 (ν(C—N)). Anal. Calc. (%) (for $C_{15}H_9CuN_5O_{10}$): C 37.32, H 1.88, N 14.51; Found: C 37.28, H 1.83, N 14.55.

Data for complex 4: Similar to the process of synthesis of complex **3**, $\mathbf{L^1}$ was replaced by $\mathbf{L^2}$ (0.0295 g), then heated at 40 °C to obtain complex **4**. Yield 68%. ESI-MS: *m/z* 419.97 $[Cu(\mathbf{L^2})(NO_3)]^+$, *m/z* 497.97 $[Cu(\mathbf{L^2})(NO_3) + DMSO]^+$; Selected IR (KBr, cm^{-1}): 3086 (ν(Ar—H)); 1583 (ν(C=N); 1526 ($\nu_{as}(NO_2)$); 1295 ($\nu_s(NO_2)$); 1384 ($\nu(NO_3^-)$); 859 (ν(C—N)). Anal. Calc. (%) (for $C_{15}H_9CuN_5O_{10}$): C 37.32, H 1.88, N 14.51; Found: C 37.29, H 1.85, N 14.48.

Data for complex 5: 0.5 mmol $CuCl_2{\cdot}2H_2O$ (0.0855 g), 0.5 mmol $\mathbf{L^3}$ (0.1650 g), methanol (15.0 mL) and chloroform (5.0 mL) were placed into a 25 mL Teflon-lined autoclave. The mixture was sealed, and then heated at 60 °C for 3 days. The mixture was slowly cooled to room temperature at a rate of 5 °C/h and filtered. The green crystal was then crystallized through slow evaporation. The blue block crystals suitable for single crystal X-ray diffraction analysis were obtained after two weeks, yield 71%. ESI-MS: *m/z* 505.89 $[Cu(\mathbf{L^3})Cl + DMSO]^+$. Selected IR (KBr, cm^{-1}): 3058; 2914(ν(Ar—H)); 1572 (ν(C=N); 829 (ν(C—Br)). Anal. Calc. (%) (for $C_{15}H_9BrCl_2CuN_2O_2$): C 38.86, H 1.96, N 6.04; Found: C 38.82, H 1.91, N 6.07.

Data for complex 6: Complex **6** was synthesized, as blue block crystals, with mixture of $CuBr_2$ (0.1 mmol, 0.0223 g), $\mathbf{L^3}$ (0.1 mmol, 0.0330 g), methanol (0.60 mL) and chloroform (0.20 mL), heated at 60 °C. Yield 65%. ESI-MS: *m/z* 471.83 $[Cu(\mathbf{L^3})Br]^+$, *m/z* 549.84 $[Cu(\mathbf{L^3})Br + DMSO]^+$; Selected IR (KBr, cm^{-1}): 3081 (ν (Ar—H)); 1572

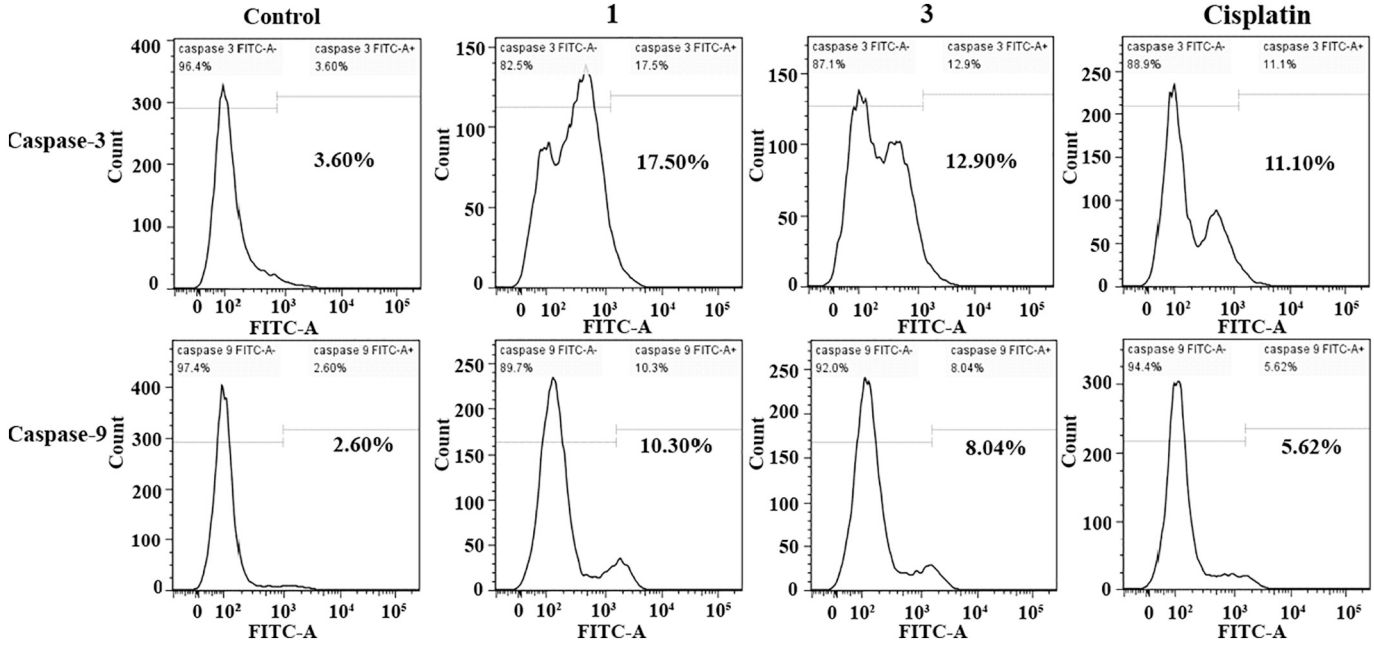

Fig. 13. The activation of caspase-3 and caspase-9 in HeLa cells treated with complex **1** (5 μM) and **3** (10.0 μM) for 24 h.

(ν(C=N); 833 (ν(C—Br)). Anal. Calc. (%) (for $C_{15}H_9Br_3CuN_2O_2$): C 32.61, H 1.64, N 5.07; Found: C 32.57, H 1.60, N 5.11.

Data for complex 7: According to the synthesis of complex **6**, $CuBr_2$ (0.1 mmol, 0.0223 g) was replaced by $Cu(NO_3)_2{\cdot}2H_2O$ (0.1 mmol, 0.0223 g), finally heated at 80 °C. The blue block crystals of complex **7** were used for single crystal X-ray diffraction analysis. Yield (75%): ESI-MS: *m/z* 454.90 $[Cu(\mathbf{L^3})(NO_3)]^+$; Selected IR (KBr, cm^{-1}): 3091 (ν(Ar—H); 1576 (ν(C=N); 1383 ($\nu(NO_3^-)$); 849 (ν(C—Br)). Anal. Calc. (%) (for $C_{15}H_9BrCuN_4O_8$): C 34.87, H 1.76, N 10.84; Found: C 34.84, H 1.71, N 10.89.

4.3. Materials and instrumentation

The data collections of single crystals of $\mathbf{L^1}$ -$\mathbf{L^2}$ and complexes **1–7** were carried out on a SuperNova CCD diffractometer or Bruker SMART Apex II CCD diffractometer equipped with graphite monochromated Mo-Ka radiation (λ = 0.710 73 Å) at room temperature. All structures were solved with direct methods by SHELX-97 programs and refined using full-matrix least-squares methods with anisotropic thermal parameters for non-hydrogen atoms on F^2 [77–79]. The crystallographic data and refinement details are summarized in Tables S1 − S4 (Supporting Information). The inhibitory rates (%) of $\mathbf{L^1}$-$\mathbf{L^3}$, $CuCl_2{\cdot}2H_2O$, $Cu(NO_3)_2{\cdot}2H_2O$, $CuBr_2$, cisplatin and newly synthesized complexes **1–7** against six cancer cells and one normal liver cell lines for 48 h are listed in Table S5. The MTT assay, cell apoptosis, measurement of $\Delta\psi_m$ analysis by JC-1 staining, ROS generation, Ca^{2+} fluctuation, RNA extraction, RT-PCR and Western blot assay of complexes **1** and **3**, were similar to those reported by Reed, Qin and Cao [25,27,65,80]. The TRAP-silver staining assay was performed using the methods reported by Reed, Qin and Deng [25,27,73]. The detailed procedures of these experimental methods were given in the supporting materials.

4.4. Statistical analysis

The data were assessed by Student's *t*-test using SPSS 13.0, p values of < 0.05 were considered statistically significant.

Abbreviations

ESI-MS	electrospray ionization mass spectroscopy
T24	human bladder cell line
MGC–80–3	human gastric cancer cell line
HeLa	human cervical cell line
Hep-G2	human hepatocellular carcinoma cell line
A549	human lung cancer cell line
SK-OV-3	human ovarian carcinoma cell line
HL-7702	human normal liver cell line
DMSO	dimethyl sulfoxide
PBS	phosphate buffer saline
TBS	Tris-HCl buffer solution
UV–vis	UV–visible
MTT	3-(4,5-dimethylthiazol-2-yl)-2,5-diphenyltetrazolium bromide
Cisplatin	diaminodichloroplatinum(II)
PI	propidium iodide
hTERT	human telomerase reverse transcriptase
ROS	reactive oxygen species
DCFH-DA	2′,7′-dichlorohydrofluorescein diacetate
JC-1	5,5′,6,6′-tetra-chloro-1,1′,3,3′-tetra-ethylbenzimidazolylcarbocyanine
$\Delta\psi_m$	mitochondrial membrane potential

Acknowledgement

This work was supported by the National Natural Science Foundation of China (Grants 81473102, 21431001), IRT_16R15, and Natural Science Foundation of Guangxi Province (Grant 2016GXNSFGA380005) as well as “BAGUI Scholar” program of Guangxi Province of China. The project was also funded by State Key Laboratory for the Chemistry and Molecular Engineering of Medicinal Resources (Guangxi Normal University), Ministry of Science and Technology of China (CMEMR2014-B13) and the Scientific Research Foundation of Hunan Provincial Education Department (Grant No.17C1421). The work also supported by University Students Innovation and Entrepreneurship Training Program Project of Guangxi (201810602256).

Appendix A. Supplementary data

The solution stability and solubility experiments, ESI-MS, ^{1}H NMR, , IR, and crystal data was listed. In addition, CCDC Nos. 1890983, 1890984 and 1890976 − 1890982 for $\mathbf{L^1}$, $\mathbf{L^2}$ and complexes **1** − **7** contains the supplementary crystallographic data for this paper. Supplementary data to this article can be found online at https://doi.org/10.1016/j.jinorgbio.2019.110820.

References

[1] D. Sun, B. Thompson, B.E. Cathers, M. Salazar, S.M. Kerwin, J.O. Trent, T.C. Jenkins, S. Neidle, L.H. Hurley, J. Med. Chem. 40 (1997) 2113–2116.
[2] T. Simonsson, P. Pecinka, M. Kubista, Nucleic Acids Res. 26 (1998) 1167–1172.
[3] A.M. Zahler, J.R. Williamson, T.R. Cech, D.M. Prescott, Nature 350 (1991) 718–720.
[4] S.N. Georgiades, N.H. Abd Karim, K. Suntharalingam, R. Vilar, Angew. Chem. Int. Ed. 49 (2010) 4020–4034.
[5] H.M. Lee, D.S.H. Chan, F. Yang, H.Y. Lam, S.C. Yan, C.M. Che, D.L. May, C.H. Leungy, Chem. Commun. 46 (2010) 4680–4682.
[6] S. Balasubramanian, L.H. Hurley, S. Neidle, Nat. Rev. Drug Discov. 10 (2011) 261–275.
[7] N.W. Kim, M.A. Piatyszek, K.R. Prowse, C.B. Harley, M.D. West, P.L.C. Ho, G.M. Coviello, W.E. Wright, S.L. Weinrich, J.W. Shay, Science 266 (1994) 2011–2015.
[8] W.C. Hahn, S.A. Stewart, M.W. Brooks, S.G. York, E. Eaton, A. Kurachi, R.L. Beijersbergen, J.H.M. Knoll, M. Meyerson, R.A. Weinberg, Nat. Med. 5 (1999) 1164–1170.
[9] T.M. Nakamura, G.B. Morin, K.B. Chapman, S.L. Weinrich, W.H. Andrews, J. Lingner, C.B. Harley, T.R. Cech, Science 277 (1997) 955–959.
[10] C.V. Dang, L.M.S. Resar, E. Emison, S. Kim, Q. Li, J.E. Prescott, D. Wonsey, K. Zeller, Exp. Cell Res. 253 (1999) 63–77.
[11] T.M. Ou, J. Lin, Y.J. Lu, J.Q. Hou, J.H. Tan, S.H. Chen, Z. Li, Y.P. Li, D. Li, L.Q. Gu, Z.S. Huang, J. Med. Chem. 54 (2011) 5671–5679.
[12] W.E. Wright, J.W. Shay, M.A. Piatyszek, Nucleic Acids Res. 23 (1995) 3794–3795.
[13] B.S. Herbert, A.E. Pitts, S.I. Baker, S.E. Hamilton, W.E. Wrigh, J.W. Shay, D.R. Corey, PNAS 96 (1999) 14276–14281.
[14] L. Harrington, W. Zhou, T. McPhail, R. Oulton, D.S.K. Yeung, V. Mar, M.B. Bass, M.O. Robinson, Genes Dev. 11 (1997) 3109–3115.
[15] B.S. Herbert, A.E. Hochreiter, W.E. Wright, J.W. Shay, Nat. Protoc. 1 (2006) 1583–1590.
[16] S.K. Noureini, H. Esmaeili, F. Abachi, S. Khiali, B. Islam, M. Kuta, A.A. Saboury, M. Hoffmann, J. Sponer, G. Parkinson, S. Haider, Biochim. Biophys. Acta Gen. Subj. 1861 (2017) 2020–2030.
[17] M. Franceschin, L. Rossetti, A. D'Ambrosio, S. Schirripa, A. Bianco, G. Ortaggi, M. Savino, C. Schultes, S. Neidle, Bioorg. Med. Chem. Lett. 16 (2006) 1707–1711.
[18] Y. Ma, T.M. Ou, J.H. Tan, J.Q. Hou, S.L. Huang, L.Q. Gu, Z.S. Huang, Eur. J. Med. Chem. 46 (2011) 1906–1913.
[19] F. Koeppel, J.F. Riou, A. Laoui, P. Mailliet, P.B. Arimondo, D. Labit, O. Petitgenet, C. Helene, J.L. Mergny, Nucleic Acids Res. 29 (2001) 1087–1096.
[20] T.M. Ou, Y.J. Lu, C. Zhang, Z.S. Huang, X.D. Wang, J.H. Tan, Y. Chen, D.L. Ma, K.Y. Wong, J.C. Tang, A.S. Chan, L.Q. Gu, J. Med. Chem. 50 (2007) 1465–1474.
[21] X.D. Wang, T.M. Ou, Y.J. Lu, Z. Li, Z. Xu, C. Xi, J.H. Tan, S.L. Huang, L.K. An, D. Li, L.Q. Gu, Z.S. Huang, J. Med. Chem. 53 (2010) 4390–4398.
[22] Y.T. Duan, Y.F. Yao, D.J. Tang, N.J. Thumar, S.B. Teraiya, J.A. Makawana, Y.L. Sang, Z.C. Wang, X.X. Tao, A.Q. Jiang, H.L. Zhu, RSC Adv. 4 (2014) 20382–20392.
[23] S. Maiti, P. Saha, T. Das, I. Bessi, H. Schwalbe, J. Dash, Bioconjug. Chem. 29 (2018) 1141–1154.
[24] M. Maiti, G.S. Kumar, J. Nucleic Acids 1 (2010) 1–24.
[25] J.E. Reed, A.A. Arnal, S. Neidle, R. Vilar, J. Am. Chem. Soc. 128 (2006) 5992–5993.
[26] A. Ali, M. Kamra, S. Roy, K. Muniyappa, S. Bhattacharya, Bioconjug. Chem. 28 (2017) 341–352.
[27] Q.P. Qin, T. Meng, M.X. Tan, Y.C. Liu, X.J. Luo, B.Q. Zou, H. Liang, Eur. J. Med. Chem. 143 (2018) 1597–1603.
[28] D. Monchaud, P. Yang, L. Lacroix, M.P. Teulade-Fichou, J.L. Mergny, Angew. Chem. Int. Ed. 47 (2008) 4858–4861.
[29] D. Griffith, J.P. Parker, C.J. Marmion, Anti Cancer Agents Med. Chem. 10 (2010)

354–370.
[30] Z.F. Chen, Q.P. Qin, J.L. Qin, J. Zhou, Y.L. Li, N. Li, Y.C. Liu, H. Liang, J. Med. Chem. 58 (2015) 4771–4789.
[31] R. Kieltyka, P. Englebienne, J. Fakhoury, C. Autexier, N. Moitessier, H.F. Sleiman, J. Am. Chem. Soc. 130 (2008) 10040–10041.
[32] Z.F. Chen, Q.P. Qin, J.L. Qin, Y.C. Liu, K.B. Huang, Y.L. Li, T. Meng, G.H. Zhang, Y. Peng, X.J. Luo, H. Liang, J. Med. Chem. 58 (2015) 2159–2179.
[33] D. Colangelo, A.L. Ghiglia, I. Viano, G. Cavigiolio, D. Osella, Biometals 16 (2003) 553–560.
[34] C.Y. Kuo, M.J. Wu, C.C. Lin, Eur. J. Med. Chem. 45 (2010) 55–62.
[35] W. Zhang, J.F. Hu, W.W. Lv, Q.C. Zhao, G.B. Shi, Molecules 17 (2012) 12950–12960.
[36] A. Bermejo, I. Andreu, F. Suvire, S. Léonce, D.H. Caignard, P. Renard, A. Pierré, R.D. Enriz, D. Cortes, N. Cabedo, J. Med. Chem. 45 (2002) 5058–5068.
[37] M.C. Linder, Biochemistry of Copper, Plenum Press, New York, 1991.
[38] C. Marzano, M. Pellei, F. Tisato, C. Santini, Anti Cancer Agents Med. Chem. 9 (2009) 185–211.
[39] G.B. Bagihalli, P.G. Avaji, S.A. Patil, P.S. Badami, Eur. J. Med. Chem. 43 (2008) 2639–2649.
[40] X.C. Shi, H.B. Fang, Y. Guo, H. Yuan, Z.J. Guo, X.Y. Wang, J. Inorg. Biochem. 190 (2019) 38–44.
[41] A. Gupte, R.J. Mumper, Cancer Treat. Rev. 35 (2009) 32–46.
[42] K.G. Daniel, P. Gupta, R.H. Harbach, W.C. Guida, Q.P. Dou, Biochem. Pharmacol. 67 (2004) 1139–1151.
[43] K.K. Jovanović, M. Tanić, L. Lvanović, N. Gligorijević, B.P. Dojčinović, S. Radulović, J. Inorg. Biochem. 163 (2016) 362–373.
[44] G. Cavigiolio, L. Benedetto, E. Boccaleri, D. Colangelo, L. Viano, D. Osella, Inorg. Chim. Acta 305 (2000) 61–68.
[45] T.M. Khan, N.S. Gul, X. Lu, R. Kumar, M.I. Choudhary, H. Liang, Z.F. Chen, Dalton Trans. 48 (2019) 11469–11479.
[46] Z.F. Chen, Y.C. Liu, L.M. Liu, H.S. Wang, S.H. Qin, B.L. Wang, H.D. Bian, B. Yang, H.K. Fun, H.G. Liu, H. Liang, C. Orvig, Dalton Trans. (2009) 262–272.
[47] Z.F. Chen, Y.F. Shi, Y.C. Liu, X. Hong, B. Geng, Y. Peng, H. Liang, Inorg. Chem. 51 (2012) 1998–2009.
[48] K.B. Huang, Z.F. Chen, Y.C. Liu, M. Wang, J.H. Wei, X.L. Xie, J.L. Zhang, K. Hu, H. Liang, Eur. J. Med. Chem. 70 (2013) 640–648.
[49] K.B. Huang, H.Y. Mo, Z.F. Chen, J.H. Wei, Y.C. Liu, H. Liang, Eur. J. Med. Chem. 100 (2015) 68–76.
[50] K.B. Huang, Z.F. Chen, Y.C. Liu, X.L. Xie, H. Liang, RSC Adv. 5 (2015) 81313–81323.
[51] F.Y. Wang, Q.Y. Xi, K.B. Huang, X.M. Tang, Z.F. Chen, Y.C. Liu, H. Liang, J. Inorg. Biochem. 169 (2017) 23–31.
[52] M. Wang, Z.F. Mao, T.S. Kang, C.Y. Wong, J.L. Mergny, C.H. Leung, D.L. Ma, Chem. Sci. 7 (2016) 2516–2523.
[53] C. Trefzer, M. Rengifo-Gonzalez, M.J. Hinner, P. Schneider, V. Makarov, S.T. Cole, K. Johnsson, J. Am. Chem. Soc. 132 (2010) 13663–13665.
[54] E. Nissinen, I.B. Linden, E. Schuitz, P. Pohto, Naunyn Schmiedeberg's Arch. Pharmacol. 346 (1992) 262–266.
[55] A.J. Souers, J.D. Leverson, E.R. Boghaert, S.L. Ackler, N.D. Catron, J. Chen, B.D. Dayton, H. Ding, S.H. Enschede, W.J. Fairbrother, D.C.S. Huang, S.G. Hymowitz, S. Jin, S.L. Khaw, P.J. Kovar, L.T. Lam, J. Lee, H.L. Maecker, K.C. Marsh, K.D. Mason, M.J. Mitten, P.M. Nimmer, A. Oleksijew, C.H. Park, C.M. Park, D.C. Phillips, A.W. Roberts, D. Sampath, J.F. Seymour, M.L. Smith, G.M. Sullivan, S.K. Tahir, C. Tse, M.D. Wendt, Y. Xiao, J.C. Xue, H.C. Zhang, R.A. Humerickhouse, S.H. Rosenberg, S.W. Elmore, Nat. Med. 19 (2013) 202–208.
[56] Y.H. Li, P.K. Li, M.J. Roberts, R.C. Arend, R.S. Samant, D.J. Buchsbaum, Cancer Lett. 349 (2014) 8–14.
[57] H.R. Zhang, K.B. Huang, Z.F. Chen, Y.C. Liu, Y.N. Liu, T. Meng, Q.P. Qin, B.Q. Zou, H. Liang, Med. Chem. Commun. 7 (2016) 806–812.
[58] W.Y. Zhang, Y.J. Wang, F. Du, M. He, Y.Y. Gu, L. Bai, L.L. Yang, Y.J. Liu, Eur. J. Med. Chem. 178 (2019) 401–416.
[59] F.G. Njoroge, B. Vibulbhan, P. Pinto, T.M. Chan, R. Osterman, Stacy Remiszewski, J.D. Rosario, R. Doll, V. Girijavallabhan, A.K. Ganguly, J. Org. Chem. 63 (1998) 445–451.
[60] K. Smith, G.A. El-Hiti, M.E.W. Hammond, D. Bahzad, Z.Q. Li, C. Siquet, J. Chem. Soc. Perkin Trans. 1 (2000) 2745–2752.
[61] J.Y. Hu, Y. Guo, J.A. Zhao, J.S. Zhang, Bioorg. Med. Chem. 25 (2017) 5733–5742.
[62] Y. Gou, J.L. Li, B.Y. Fan, B.H. Xu, M. Zhou, F. Yang, Eur. J. Med. Chem. 134 (2017) 207–217.
[63] H.M. Coley, J. Sarju, G. Wagner, J. Med. Chem. 51 (2008) 135–141.
[64] T. Meng, S.F. Tang, Q.P. Qin, Y.L. Liang, C.X. Wu, C.Y. Wang, H.T. Yan, J.X. Dong, Y.C. Liu, Med. Chem. Commun. 7 (2016) 1802–1811.
[65] Q.P. Qin, T. Meng, M.X. Tan, Y.C. Liu, X.J. Luo, B.Q. Zou, H. Liang, Eur. J. Med. Chem. 143 (2018) 1387–1395.
[66] K.J. Wu, C. Grandori, M. Amacker, N.S. Vermot, A. Polack, J. Lingner, R.D. Favera, Nat. Genet. 21 (1999) 220–224.
[67] G. Biffi, D. Tannahill, J. McCafferty, S. Balasubramanian, Nat. Chem. 5 (2013) 182–186.
[68] E. Eruslanov, S. Kusmartsev, Identification of ROS using oxidized DCFDA and flow cytometry, in: D. Armstrong (Ed.), Advanced Protocols in Oxidative Stress II, Methods in Molecular Biology. 594, Humana Press, New York, 2010, pp. 57–72.
[69] X.Z. Hu, Y. Xu, D.C. Hu, Y. Hui, F.X. Yang, Toxicol. Lett. 171 (2007) 19–28.
[70] Q.P. Qin, T. Meng, Z.Z. Wei, C.H. Zhang, Y.C. Liu, H. Liang, Z.F. Chen, Eur. J. Inorg. Chem. (2017) 1824–1834.
[71] D.R. Laver, Biophys. J. 92 (2007) 3541–3555.
[72] Q.P. Qin, J.L. Qin, T. Meng, W.H. Lin, C.H. Zhang, Z.Z. Wei, J.N. Chen, Y.C. Liu, H. Liang, Z.F. Chen, Eur. J. Med. Chem. 124 (2016) 380–392.
[73] J.G. Deng, P. Yu, Z.L. Zhang, J. Wang, J.H. Cai, N. Wu, H.B. Sun, H. Liang, F. Yang, Eur. J. Med. Chem. 158 (2018) 442–452.
[74] Y.L. Zhang, Q.P. Qin, Q.Q. Cao, H.H. Han, Z.L. Liu, Y.C. Liu, H. Liang, Z.F. Chen, Med. Chem. Commun. 8 (2017) 184–190.
[75] B. Antonsson, F. Conti, A.M. Ciavatta, S. Montessuit, S. Lewis, L. Martinou, L. Bernasconi, A. Bernard, J.J. Mermod, G. Mazzei, K. Maundrell, F. Gambale, R. Sadoul, J.C. Martinou, Science 277 (1997) 370–372.
[76] D. Yugandhar, V.L. Nayak, S. Archana, K.C. Shekar, A.K. Srivastav, Eur. J. Med. Chem. 101 (2015) 348–357.
[77] G.M. Sheldrick, A short history of SHELX, Acta Crystallogr. Sect. A: Found. Crystallogr. 64 (2008) 112.
[78] G.M. Sheldrick, SHELXT V. 2014/3, Program for Crystal Structure Solution, University of Göttingen, 2014.
[79] G.M. Sheldrick, v SHELXL, Program for Crystal Structure Refinement, University of Göttingen, 2014, p. 2014.
[80] R. Cao, J.L. Jia, X.C. Ma, M. Zhou, H. Fei, J. Med. Chem. 56 (2013) 3636–3644.